

Electromagnetically induced transparency and reduced speeds for single photons in a fully quantized model

Thomas Purdy

Department of Physics, Carnegie Mellon University, Pittsburgh, PA 15213

Martin Ligare*

Department of Physics, Bucknell University, Lewisburg, PA 17837

(Dated: October 25, 2018)

We introduce a simple model for electromagnetically induced transparency in which all fields are treated quantum mechanically. We study a system of three separated atoms at fixed positions in a one-dimensional multimode optical cavity. The first atom serves as the source for a single spontaneously emitted photon; the photon scatters from a three-level Λ -configuration atom which interacts with a single-mode field coupling two of the atomic levels; the third atom serves as a detector of the total transmitted field. We find an analytical solution for the quantum dynamics. From the quantum amplitude describing the excitation of the detector atom we extract information that provides exact single-photon analogs to wave delays predicted by semi-classical theories. We also find complementary information in the expectation value of the electric field intensity operator.

I. INTRODUCTION

Controlling the phase coherence in ensembles of multilevel atoms has led to the observation of many striking phenomena in the propagation of near-resonant light. These phenomena include coherent population trapping, lasing without inversion, electromagnetically induced transparency, and anomalously slow and anomalously fast pulse velocities. Resonant enhancement of the index of refraction without accompanying increased in absorption was proposed [1] and observed [2, 3] in 1991, and drastic reductions in the group velocity of pulses were discussed shortly thereafter [4]. Recent experiments have taken the reduction of the speed of light to extreme limits [5, 6] and at the other extreme lie observations of seemingly superluminal light [7, 8]. An overview of recent developments in the control of photons is presented in Ref. [9]. An earlier review of electromagnetically induced transparency was presented by Harris [10], while Lukin et al. present a overview of phase coherence in general, with an extensive list of references [11]. Such effects are also discussed in a recent texts (see, for example, Ref. [12]). In most previous work the phenomenon of electromagnetically induced transparency and the accompanying drastic slowing of the speed of light are treated using semi-classical theory in which the atoms of the medium are treated quantum mechanically and the fields are treated classically. We use a model in which the entire system is treated quantum mechanically, and study the propagation of a field state containing a single photon. Although coherent states of a single mode quantized field are often considered as the “most classical,” the single photon states that we study exhibit striking parallels with classical fields.

We study a system of three separated atoms at fixed positions in a one-dimensional multimode optical cavity. The first atom serves as the source for a single spontaneously emitted photon; the photon scatters from a three-level Λ -configuration atom which interacts with an additional single-mode field coupling two of the atomic levels; and the third atom serves as a detector of the total transmitted field. In the spirit of Feynman’s derivation of the classical index of refraction from the interaction of a field with a single oscillator [13], we infer the properties of a medium exhibiting electromagnetically induced transparency from the interaction of the spontaneously emitted quantum field with the single quantized scattering atom. We find an analytical solution for the quantum dynamics, including reradiation from the scatterer, and from this we deduce quantum delays that characterize the propagation of the field. These delays are equivalent to those predicted by semi-classical theories. In our quantum model all delays are clearly the result of interfering amplitudes that reshape the temporal envelope of the probability of detecting the transmitted photon. This effect is most clearly illustrated in the graphs of detection probability vs. time displayed in Sec. V. This work is an extension of the model we have used previously to study quantum manifestations of classical wave delays induced by scattering from simple two-level atoms [14]. We note that the analytical results obtained in this paper may be verified using the straightforward numerical techniques like those used in Refs. [15, 16, 17, 18].

II. REVIEW OF SEMI-CLASSICAL THEORY

Electromagnetically induced transparency can be observed in the simple three-level atom illustrated in Fig. 1. A strong laser “coupling” laser with angular frequency ω_c is tuned to resonance with the transition between atomic levels B and C, while a weak “probe” laser with angular frequency ω_p excites the transition between levels A and

*mligare@bucknell.edu

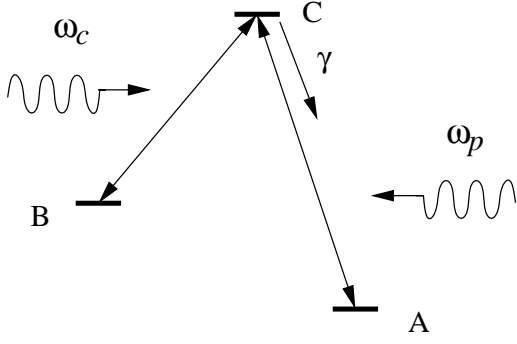


FIG. 1: Level scheme for simple electromagnetically induced transparency. A strong field resonantly couples levels B and C, and weak probe is near resonance with the transition between levels A and C. The upper level C decays via spontaneous emission at a rate γ to the ground state A. All other damping mechanisms are assumed to be negligible.

C. In this paper we consider the simplest case in which decay from level C to B is small enough to be neglected, and the only damping is due to emission at a rate γ from level C to the ground state A. (In this paper all decay rates γ_j refer to decay of *probability* of finding the atom in the excited state.) We also assume that there is no incoherent pumping driving population between the levels of the atom.

In the limit of a weak probe, the complex susceptibility is given by [12]

$$\chi = \left(\frac{N|d|^2}{\hbar\epsilon_0} \right) \frac{\delta}{\omega_R^2/4 - \delta^2 - i\delta\gamma/2}, \quad (1)$$

where N is the density of the atoms, d is the dipole moment of the transition between levels A and C, ω_R is the Rabi frequency of the coupling transition between levels B and C, and the detuning of the probe laser frequency from resonance is

$$\delta = \omega_p - \omega_{AC}. \quad (2)$$

The real and imaginary parts of the susceptibility are illustrated in Fig. 2 for a coupling field strength such that $\omega_R = \gamma/2$. The index of refraction and the absorption coefficient can be calculated from the real and imaginary parts of the complex susceptibility respectively. When the probe field is resonant with the transition between levels A and C, i.e., $\delta = 0$, the absorption goes to zero and the index of refraction is a rapidly varying function of probe frequency.

For later comparison with the results of our quantum model, we consider a classical monochromatic plane wave of frequency ω which is normally incident on a thin slab containing atoms with the level structure illustrated in Fig. 1. The plane of the slab is normal to the z axis, the thickness of the slab is Δz , and the density of the atoms is N . If the incident field is $E_i = E_0 e^{-i\omega(t-z/c)}$, the transmitted field on the far side of the slab is

$$E_t = E_i e^{i\omega\chi\Delta z/(2c)}, \quad (3)$$

and for weak scattering the transmitted field is approximately

$$\begin{aligned} E_t &\simeq E_i \left(1 + i \frac{\omega\Delta z}{2c} \chi \right) \\ &= E_i \left[1 + i \left(\frac{N\Delta z|d|^2\omega}{\hbar\epsilon_0 c\gamma} \right) \frac{\delta\gamma/2}{\omega_R^2/4 - \delta^2 - i\delta\gamma/2} \right] \end{aligned} \quad (4)$$

The scattering is characterized by the dimensionless parameter $N\Delta z|d|^2\omega/(\hbar\epsilon_0 c\gamma)$.

The dispersion in the response of the atoms in this model leads to delays of pulses traversing such a slab. The delay in the arrival of the peak of a modulation envelope of a quasi-monochromatic pulse that is away from a region of anomalous dispersion is determined by the group velocity $v_g = d\omega/dk = c/(n + \omega \frac{dn}{d\omega})$, and is given by

$$\begin{aligned} \Delta t_g &= \frac{\Delta z}{v_g} - \frac{\Delta z}{c} \\ &= \frac{\Delta z}{c} \left(n - 1 + \omega \frac{dn}{d\omega} \right). \end{aligned} \quad (5)$$

For detunings such that $\delta \ll \omega_{AC}$ the group delay is

$$\begin{aligned} \Delta t_g &= \left(\frac{2N\Delta z|d|^2\omega_{AC}}{\hbar\epsilon_0 c} \right) \\ &\times \frac{(\omega_R^2 + 4\delta^2) [(\omega_R^2 - 4\delta^2)^2 - 4\gamma^2\delta^2]}{[(\omega_R^2 - 4\delta^2)^2 + 4\gamma^2\delta^2]^2}. \end{aligned} \quad (6)$$

The functional form of the delay when $\omega_R = \gamma/2$ is illustrated in Fig. 3. When the probe field is resonant with the transition between levels A and C, not only is the absorption zero, but the group velocity can be extremely

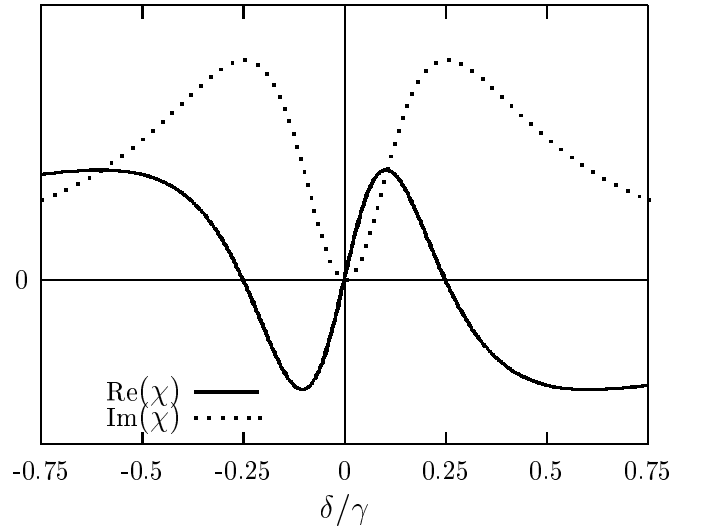


FIG. 2: Real and imaginary parts of the complex susceptibility for the three-level system illustrated in Fig. 1. The strength of the coupling field is such that $\omega_R = \gamma/4$.

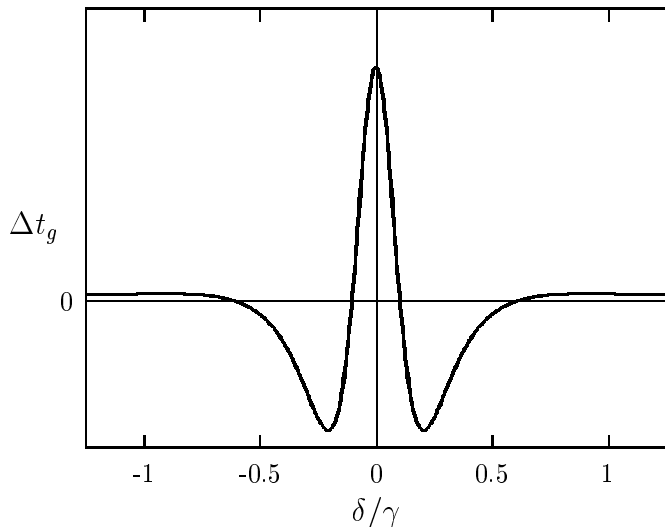


FIG. 3: Group delay for a classical pulse in a medium with susceptibility given by Eq. (1). As in Fig. 2, the strength of the coupling field is such that $\omega_R = \gamma/2$.

small, and this is manifested in the large positive group delay at $\delta = 0$ in Fig. 3. The central peak in Fig. 3 becomes taller and narrower as the strength of the coupling field is reduced. We note that for some values of the detuning δ the group delay is negative, which corresponds to group velocities greater than the vacuum speed of light c . Such “superluminal” velocities do not violate causality, and are an effect of pulse reshaping by the dispersive medium. Similar reshaping effects and group velocities greater than c occur near simple two-level resonances in both classical and quantum theories [14].

For pulses that are either not sufficiently monochromatic, or not sufficiently far away from a region of anomalous dispersion, the simple concepts of phase and group velocity are inadequate to characterize all of the effects of pulse-reshaping as a field propagates. Several other velocities and delays have been developed (see, for example, Refs. [19, 20]) and in this paper we focus on a delay determined by the “temporal center of gravity” of the field intensity of a pulse at a fixed position z “downstream” from the slab containing the atoms comprising the medium, i.e.,

$$\Delta t_{\mathcal{E}^2} = \left(\frac{\int t \mathcal{E}(z, t)^2 dt}{\int \mathcal{E}(z, t)^2 dt} \right)_{\text{after medium}} - \left(\frac{\int t \mathcal{E}(z, t)^2 dt}{\int \mathcal{E}(z, t)^2 dt} \right)_{\text{vacuum}}. \quad (7)$$

This is closely related to concepts used to define the centroid velocity in [19]. We have investigated this delay in classical and quantum mechanical models of scattering from simple two-level atoms in a previous paper [14]. For quasi-monochromatic pulses far from resonance this delay is equivalent to the group delay, but in general it is

necessary to calculate explicitly the field \mathcal{E} in order to determine $\Delta t_{\mathcal{E}^2}$. For the specific fields considered in this paper we will show that the “temporal-center-of-gravity” delay happens to be equal to twice the group delay.

III. QUANTUM MECHANICAL MODEL

The quantum mechanical system we consider is illustrated in Fig. 4, and consists of three atoms in a multimode one-dimensional optical cavity that extends from $z = 0$ to $z = L$. This multimode cavity is oriented horizontally in the schematic representation of Fig. 4. The middle atom has an additional interaction with a single-mode field contained in the vertical cavity. The field in the multimode (horizontal) cavity plays the role of the probe field, and the field in the single mode (vertical) cavity represents the coupling field. (The finite optical cavities do not contribute to the physical phenomena under investigation; they simply provide a convenient quantization volume for the field modes used in our calculation.) In the remainder of this section we will discuss the details of our model and the standard quantum optical Hamiltonian we use. We also present the analytical solution for the time dependence of the system.

The atom on the left (atom 1) is a two-level atom which is initially in the excited state, and will be the source of the probe field. The middle atom (atom 2) which will scatter the radiation emitted by the source is a three-level atom with the “lambda” configuration of Fig. 1, with the energy difference between levels A and C close to that of the level separation of atom 1. (The highest level of all three atoms will be labeled as C.) Levels B and C of atom 2 will interact with the single-mode coupling field which is assumed to be exactly on resonance. The coupling field will initially be in a state with a well-defined number of photons such that the Rabi frequency of the transition

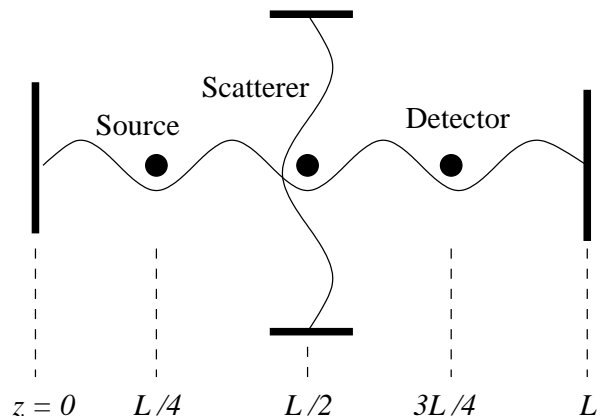


FIG. 4: Quantum mechanical model consisting of three atoms at fixed positions. All three atoms interact with the radiation in the probe field in the *multimode* cavity (represented horizontally) and the middle atom also interacts with the single mode coupling field (represented vertically).

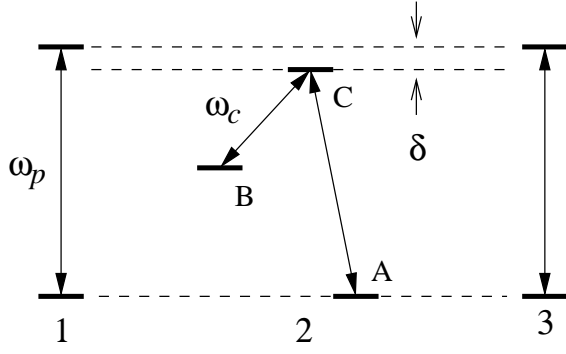


FIG. 5: Level scheme of the source, scattering, and detector atoms. The source and detector are two-level atoms with identical transition frequencies. The scattering atom is a three-level atom in the Λ configuration. The transition frequency of the source and detector are detuned from the A-C transition of the scattering atom by an amount δ .

between levels B and C is appropriate for the observation of electromagnetically induced transparency. The two-level atom on the right (atom 3) will serve as a detector. The detector atom is assumed to have the same resonant frequency as the source atom. The relative energy levels of all three atoms are illustrated in Fig. 5.

We assume that the coupling strengths of the atoms to the probe field are all independent, so that the atoms have separate spontaneous decay rates. Although we find a solution for the dynamics for any decay rates, we focus our attention in this paper on cases in which the decay rate of atom 1 is very much smaller than the decay rate of atom 2. This condition insures that the spectrum of the radiation emitted by atom 1 will be very much narrower than the linewidth of the the scattering atom, and this allows us to compare our results from the quantum case with those of the semi-classical model which assumes that the sample is driven by a monochromatic wave. We also assume that the decay rate of the detector atom (atom 3) is very much greater than any other dynamical rates in the problem. In this limit the excitation of atom 3 will closely follow the field drives it. For simplicity we also assume that the spontaneous decay rate from level C to level B (for atom 2) is negligible.

The zero-field resonance frequencies of the A-C transitions of the atoms are labeled $\omega_j^{(\text{at})}$, where $j = 1, 2$, or 3 , and the positions of the atoms will be labeled z_j . In the remainder of the paper we will assume that the atoms are at positions $z_1 = L/4$, $z_2 = L/2$, and $z_3 = 3L/4$, as illustrated in Fig. 4, although our results for delay times do not depend on the exact positions. The standing wave field modes of the probe field cavity are separated in angular frequency by the fundamental frequency

$$\Delta = \pi \frac{c}{L}. \quad (8)$$

This mode spacing may be small enough that many modes fall within the natural line-width of the atoms.

For convenience we assume that the frequency of one of the modes corresponds exactly to the resonance frequency of atom 1, the emitting atom, and that the length of the cavity is such that it contains an even number of wavelengths of this mode. We label the frequency of this mode $\omega_0 = k_0 \Delta$, where k_0 is an integer divisible by 4. (This assumption affects the details of some of our calculations, but not our results concerning delay times.) The other mode frequencies will be enumerated from this mode so that

$$\omega_k = (k_0 + k) \Delta, \quad (9)$$

where $k = 0, \pm 1, \pm 2, \dots$

As in the semi-classical case we wish to study the effects of the detuning of the source field on the scattering of the radiation. We use the same symbol δ as in the semi-classical case to represent the detuning of the field, but in the quantum case the detuning is directly tied to the properties of the source and scattering atoms:

$$\delta = \omega_1^{(\text{at})} - \omega_2^{(\text{at})}. \quad (10)$$

Because the detector atom is assumed to have the same resonance frequency as the source atom we have $\omega_1^{(\text{at})} = \omega_3^{(\text{at})}$.

We use as basis states the eigenstates of the atomic plus free-field Hamiltonian

$$\begin{aligned} \hat{H}_0 &= \hat{H}_{\text{atoms}} + \hat{H}_{\text{field}} \\ &= \hat{H}_{\text{atoms}} + \hat{H}_{\text{probe}} + \hat{H}_{\text{coupling}} \\ &= \hbar \omega_1^{(\text{at})} |C_1\rangle \langle C_1| + \hbar \omega_2^{(\text{at})} |C_2\rangle \langle C_2| + \hbar (\omega_2^{(\text{at})} - \omega_c) |B_2\rangle \langle B_2| + \hbar \omega_3^{(\text{at})} |C_3\rangle \langle C_3| + \sum_k \hbar \omega_k a_k^\dagger a_k + \hbar \omega_c a_c^\dagger a_c, \end{aligned} \quad (11)$$

where a_k and a_k^\dagger are the lowering and raising operators for the k^{th} mode of the probe field, and a_c and a_c^\dagger act similarly on the single mode of the coupling field. (We

have re-zeroed the energy scale to remove zero-point energy of the field modes.) The basis states will be denoted as follows:

- $|C, A, A; \emptyset, N\rangle$ — Atom 1 excited, atoms 2 and 3 in the ground state, no photons in the cavity modes, N photons in the coupling mode;
- $|A, C, A; \emptyset, N\rangle$ — Atom 2 in state C, atoms 1 and 3 in the ground state, no photons in the probe field, N photons in the coupling mode;
- $|A, A, C; \emptyset, N\rangle$ — Atom 3 excited, atoms 1 and 2 in the ground state, no photons in the probe field, N photons in the coupling mode;
- $|A, A, A; 1_k, N\rangle$ — All atoms in the ground state, one photon in the probe field mode with frequency $(k_0 + k)\Delta$, N photons in the coupling mode;
- $|A, B, A; \emptyset, N + 1\rangle$ — Atom 2 in state B, atoms 1 and 3 in the ground state, $N + 1$ photons in the coupling field.

Each atom is coupled to all of the standing wave modes of the probe field, and we use the symbol g_{jk} to label the coefficients characterizing the strength of the coupling of the j^{th} atom to the k^{th} mode of the probe field. In addition atom 2 interacts with the coupling field, and this interaction is characterized by the constant g_c . We use the standard electric-dipole and rotating-wave approximation approximations to give the following interaction Hamiltonian:

$$\begin{aligned} \hat{H}_{\text{int}} = & \sum_{j=1}^3 \sum_k \hbar \left(g_{jk} a_k^\dagger |A_j\rangle \langle C_j| + g_{jk}^* a_k |C_j\rangle \langle A_j| \right) \\ & + \hbar \left(g_c a_c^\dagger |B_2\rangle \langle C_2| + \Omega_c^* a_c |C_2\rangle \langle B_2| \right). \end{aligned} \quad (12)$$

The Rabi frequency ω_R of the transition between levels B and C is determined by the number of photons in the coupling mode and the coupling constant g_c as follows:

$$\omega_R = 2g_c \sqrt{N+1}. \quad (13)$$

For convenience we assume that ω_R is real.

We assume that the frequencies of all atomic transitions are very much greater than the fundamental frequency of the cavity, that is $\omega_j^{(\text{at})} \gg \Delta$ for all atoms, and similarly for ω_c . In this limit we can make the approximation that all modes that influence the dynamics of the system are near the atomic resonances, and the atom-field coupling constants can be factored into a product of a frequency-independent constant and a space-dependent coupling factor. The coupling constants g_{jk} are given in terms of the electric dipole matrix element d_j between the levels A and C of atom j , the effective volume of the cavity, V , and the permittivity of free space, ϵ_0 , by

$$\begin{aligned} g_{jk} &= d_j \left(\frac{\omega_j^{(\text{at})}}{2\hbar\epsilon_0 V} \right) \sin[(k_0 + k)\pi z_j / L] \\ &= \Omega_j \sin[(k_0 + k)\pi z_j / L], \end{aligned} \quad (14)$$

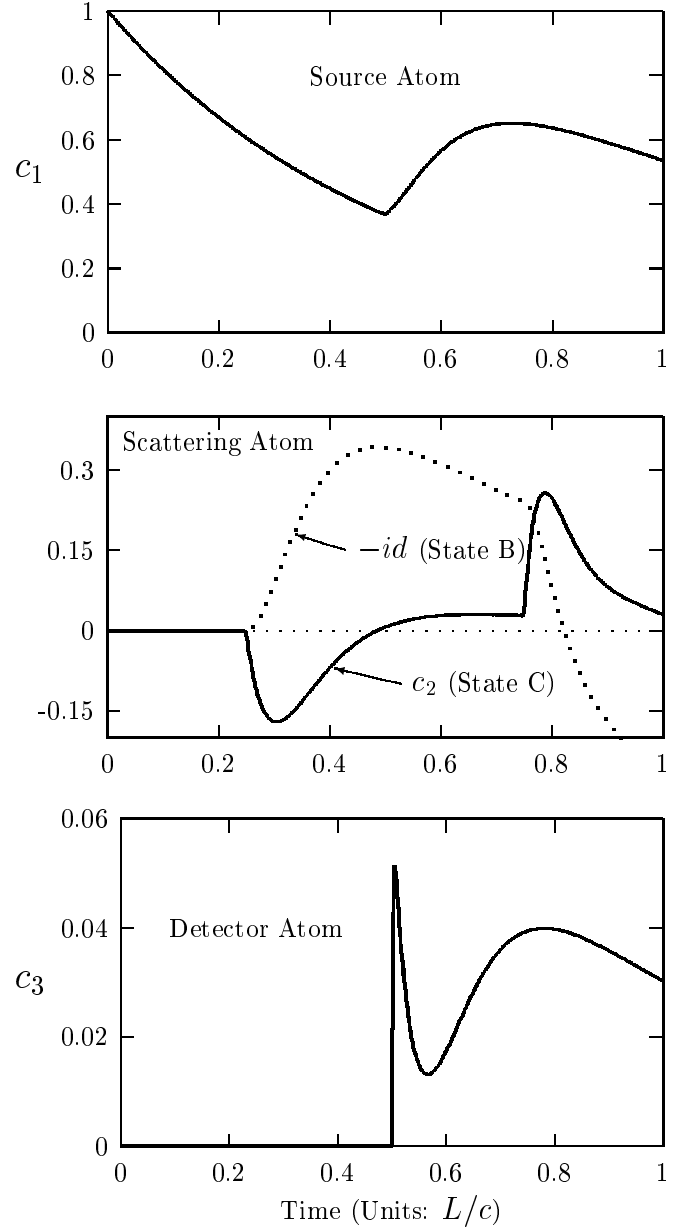


FIG. 6: Magnitude of the amplitudes for the atoms to be in the excited state, starting from the state $|\psi(0)\rangle = |e, g, g; \emptyset, N\rangle$. The decay rates of the atoms are $\gamma_1 = 4, \gamma_2 = 64$, and $\gamma_3 = 1024$; the Rabi frequency of the B-C transition of atom 2 is $\omega_R = \gamma_2/2 = 32$, and $\delta = 0$.

where in the last line we have defined the quantity

$$\Omega_j = d_j \left(\frac{\omega_j^{(\text{at})}}{2\hbar\epsilon_0 V} \right), \quad (15)$$

which is independent of the cavity mode-frequency.

We write the state of the system as the linear combination

$$\begin{aligned} |\psi(t)\rangle = & c_1(t)|C, A, A; \emptyset, N\rangle + c_2(t)|A, C, A; \emptyset, N\rangle \\ & + c_3(t)|A, A, C; \emptyset, N\rangle \end{aligned}$$

$$+d(t)|A, B, A; \emptyset, N+1\rangle + \sum_k b_k(t)|A, A, A; 1_k, N\rangle. \quad (16)$$

Choosing the zero of the energy scale at the level of (uncoupled) state $|C, A, A; \emptyset, N\rangle$, the Schrödinger yields the following set of coupled differential equations:

$$\dot{c}_1 = -i \sum_k g_{1k} b_k, \quad (17)$$

$$\dot{c}_2 = -i \left(\sum_k g_{2k} b_k + \omega_R d/2 - \delta c_2 \right), \quad (18)$$

$$\dot{c}_3 = -i \sum_k g_{3k} b_k, \quad (19)$$

$$\dot{d} = -i(\omega_R c_2/2 - \delta d), \quad (20)$$

$$\dot{b}_k = -i \left(\sum_j g_{jk}^* c_j + k \Delta b_k \right). \quad (21)$$

We solve this set of equations with the Laplace transform technique used by Stey and Gibberd [21] for a Hamiltonian similar to that for a single atom at the center of one-dimensional cavity. Laplace transforms have also been used to solve the Schrödinger equation in similar problems with two interacting atoms in three-dimensions [22, 23] and in our own recent work on scattering from two-level atoms [14]. Because the Laplace transform technique is not new, and because we would like to focus on analogies with the fields in the semi-classical model and physical interpretation, we leave the details of our solution to the appendix, and simply quote our results here.

The general features of the solution giving the time-dependences of the atomic excitation amplitudes are il-

lustrated in Fig. 6. The initially excited atom decays exponentially until the time $t = 0.5L/c$ at which scattered and reflected radiation first returns to the atom. The amplitudes to find the other atoms excited are identically zero until radiation first reaches them: the scattering atom first becomes excited at $t = 0.25L/c$ and the detector atom is first excited at $t = 0.5L/c$. The three decay constants which characterize the spontaneous emission rates of level C in each of the atoms emerge naturally in terms of the parameters of the Hamiltonian as

$$\gamma_k = \frac{\pi |\Omega_k|^2}{\Delta} = |\Omega_k|^2 \frac{L}{c}. \quad (22)$$

The causal nature of the dynamics is evident in that all disturbances are propagated at the speed of light c via the quantum field. The abrupt changes in the complex amplitudes at intervals of $0.5L/c$ are a manifestation of the finite speed of light and the atomic spacing of $0.25L$.

The abrupt changes appear in our analytic solution for the complex amplitudes $c_j(t)$, $d(t)$, and $b_k(t)$ as sums of terms with step functions that “turn on” at successively later intervals of $0.5L/c$. In the following formulas giving these amplitudes we truncate the expressions so that only the first excitation of atoms 2 and 3 are included. We also note that the following equations are specific in some details to the atomic positions z_i used in this paper. The “turn-on” times and relative phases of terms will change with different positions, but the conclusions of this paper concerning delay times are unaffected by these details. The time dependence of the system is given by the following set of amplitudes, in which we use the labels \mathcal{F}_i as a shorthand for complicated factors that are functions of γ_i , δ , ω_R , and (in the case of b_k), k :

$$c_1(t) = e^{-\frac{\gamma_1}{2}t} + \Theta\left(t - \frac{1}{2}\right) \left\{ e^{-\frac{\gamma_1}{2}(t-\frac{1}{2})} \left[\mathcal{F}_1 + \left(t - \frac{1}{2}\right) \mathcal{F}_2 \right] + e^{[-(\gamma_2 - \sqrt{\gamma_2^2 - 4\omega_R^2})/4 + i\delta](t-\frac{1}{2})} \mathcal{F}_3 + e^{[-(\gamma_2 + \sqrt{\gamma_2^2 - 4\omega_R^2})/4 + i\delta](t-\frac{1}{2})} \mathcal{F}_4 \right\} + \dots \quad (23)$$

$$c_2(t) = \Theta\left(t - \frac{1}{4}\right) \left\{ e^{-\frac{\gamma_1}{2}(t-\frac{1}{4})} \mathcal{F}_5 + e^{[-(\gamma_2 - \sqrt{\gamma_2^2 - 4\omega_R^2})/4 + i\delta](t-\frac{1}{4})} \mathcal{F}_6 + e^{[-(\gamma_2 + \sqrt{\gamma_2^2 - 4\omega_R^2})/4 + i\delta](t-\frac{1}{4})} \mathcal{F}_7 \right\} + \dots \quad (24)$$

$$c_3(t) = \Theta\left(t - \frac{1}{2}\right) \left\{ e^{-\frac{\gamma_1}{2}(t-\frac{1}{2})} \mathcal{F}_8 + e^{[-(\gamma_2 - \sqrt{\gamma_2^2 - 4\omega_R^2})/4 + i\delta](t-\frac{1}{2})} \mathcal{F}_9 + e^{[-(\gamma_2 + \sqrt{\gamma_2^2 - 4\omega_R^2})/4 + i\delta](t-\frac{1}{2})} \mathcal{F}_{10} + e^{-\frac{\gamma_3}{2}(t-\frac{1}{2})} \mathcal{F}_{11} \right\} + \dots \quad (25)$$

$$d(t) = \Theta\left(t - \frac{1}{4}\right) \left\{ e^{-\frac{\gamma_1}{2}(t-\frac{1}{4})} \mathcal{F}_{12} + e^{[-(\gamma_2 - \sqrt{\gamma_2^2 - 4\omega_R^2})/4 + i\delta](t-\frac{1}{4})} \mathcal{F}_{13} + e^{[-(\gamma_2 + \sqrt{\gamma_2^2 - 4\omega_R^2})/4 + i\delta](t-\frac{1}{4})} \mathcal{F}_{14} \right\} + \dots \quad (26)$$

$$b_k(t) = \left(e^{-\frac{\gamma_1}{2}t} - e^{-ik\pi t} \right) g_{1k} \mathcal{F}_{15} + \Theta\left(t - \frac{1}{4}\right) g_{2k} \left\{ e^{-\frac{\gamma_1}{2}(t-\frac{1}{4})} \mathcal{F}_{16} + e^{-ik\pi(t-\frac{1}{4})} \mathcal{F}_{17} \right\}$$

$$+e^{[-(\gamma_2-\sqrt{\gamma_2^2-4\omega_R^2})/4+i\delta](t-\frac{1}{4})}\mathcal{F}_{18}+e^{[-(\gamma_2+\sqrt{\gamma_2^2-4\omega_R^2})/4+i\delta](t-\frac{1}{4})}\mathcal{F}_{19}\}+\dots \quad (27)$$

Complete expressions for the factors \mathcal{F}_i may be found in the appendix.

Four time scales are manifest in the exponential factors in these equations: the exponential decay rate of the source atom γ_1 , which is assumed to be small, the exponential decay rate of the detector atom γ_3 , which is assumed to be large, and two decay rates associated with the scattering atom, $(\gamma_2 + \sqrt{\gamma_2^2 - 4\omega_R^2})/2$ and $(\gamma_2 - \sqrt{\gamma_2^2 - 4\omega_R^2})/2$. When the coupling field strength is small, the last of these rates approaches zero. This means that decay from the scattering atom can be very slow, and this slow reradiation is at the origin of the reduced velocities which characterize media with electromagnetically induced transparency.

In the following sections we will focus on two quantities: $c_3(t)$, the amplitude to find the detector atom excited, and $\langle \hat{\mathcal{E}}^2 \rangle$ the expectation value of the square of the electric field operator, which is proportional to the field intensity. (The expectation value of the field operator itself is 0 for any single-photon state.) In our investi-

gation of $c_3(t)$ we will consider only the first term in Eq. (25) describing the initial excitation of the detector atom. Similarly, we will investigate $\langle \hat{\mathcal{E}}^2 \rangle$ in regions to the right the scattering atom, and at times that exclude multiple scattering effects.

It is useful to rewrite $c_3(t)$ as the sum of two pieces, the amplitude $c_3^0(t)$ for atom 3 to be excited in the absence of the scattering atom (or, equivalently, when $\gamma_2 = 0$), plus $c_3^s(t)$, the amplitude that is attributable to scattering:

$$c_3(t) \equiv c_3^0(t) + c_3^s(t). \quad (28)$$

Setting $\gamma_2 = 0$ in Eq. (25) gives

$$c_3^0(t) = \Theta\left(t - \frac{1}{2}\right) \frac{\sqrt{\gamma_1\gamma_3}}{\gamma_1 - \gamma_3} \times \left(e^{-\frac{\gamma_1}{2}(t-\frac{1}{2})} - e^{-\frac{\gamma_3}{2}(t-\frac{1}{2})}\right), \quad (29)$$

and subtracting this from Eq. (25) gives

$$c_3^s(t) = \Theta\left(t - \frac{1}{2}\right) \left\{ e^{-\frac{\gamma_1}{2}(t-\frac{1}{2})}\mathcal{F}_{20} + e^{[-(\gamma_2-\sqrt{\gamma_2^2-4\omega_R^2})/4+i\delta](t-\frac{1}{2})}\mathcal{F}_{21} + e^{[-(\gamma_2+\sqrt{\gamma_2^2-4\omega_R^2})/4+i\delta](t-\frac{1}{2})}\mathcal{F}_{22} + e^{-\frac{\gamma_3}{2}(t-\frac{1}{2})}\mathcal{F}_{23} \right\} \quad (30)$$

where

$$\mathcal{F}_{20} = \left(\frac{\sqrt{\gamma_1\gamma_3}}{\gamma_1 - \gamma_3}\right) \frac{\gamma_2(\gamma_1 + i2\delta)}{\gamma_1^2 - \gamma_1\gamma_2 - 4\delta^2 + \omega_R^2 + i2\delta(2\gamma_1 - \gamma_2)} \quad (31)$$

$$\mathcal{F}_{21} = \left(\frac{2\sqrt{\gamma_1\gamma_3}}{\sqrt{\gamma_2^2 - 4\omega_R^2}}\right) \frac{\gamma_2(\gamma_2 - \sqrt{\gamma_2^2 - 4\omega_R^2})}{(2\gamma_1 - \gamma_2 + \sqrt{\gamma_2^2 - 4\omega_R^2} + i4\delta)(2\gamma_3 - \gamma_2 + \sqrt{\gamma_2^2 - 4\omega_R^2} + i4\delta)} \quad (32)$$

$$\mathcal{F}_{22} = \left(\frac{2\sqrt{\gamma_1\gamma_3}}{\sqrt{\gamma_2^2 - 4\omega_R^2}}\right) \frac{\gamma_2(\gamma_2 + \sqrt{\gamma_2^2 - 4\omega_R^2})}{(2\gamma_1 - \gamma_2 - \sqrt{\gamma_2^2 - 4\omega_R^2} + i4\delta)(2\gamma_3 - \gamma_2 - \sqrt{\gamma_2^2 - 4\omega_R^2} + i4\delta)} \quad (33)$$

$$\mathcal{F}_{23} = \left(\frac{\sqrt{\gamma_1\gamma_3}}{\gamma_1 - \gamma_3}\right) \frac{\gamma_2(\gamma_3 + i2\delta)}{\gamma_3^2 - \gamma_2\gamma_3 - 4\delta^2 + \omega_R^2 + i2\delta(2\gamma_3 - \gamma_2)} \quad (34)$$

In our investigations of the quantum field itself we use the electric field operator in the form given by Meystre and Sargent [24], and write the expectation value of the square of the field as

$$\langle \hat{\mathcal{E}}^2 \rangle = \langle \psi(t) | \left\{ \sum_k \sqrt{\frac{\hbar\omega_k}{\epsilon_0 V}} (a_k + a_k^\dagger) \sin\left[(k_0 + k)\frac{\pi z}{L}\right] \right\}^2 | \psi(t) \rangle. \quad (35)$$

In the limit considered in this paper we can replace

the frequencies ω_k under the radical with the constant

$\omega_1^{(\text{at})}$. After expanding the state vector as in Eq. (16) and evaluating the sums, the expectation value can be written in terms of the amplitudes $b_k(t)$ to find the photon in the various cavity modes:

$$\langle \hat{\mathcal{E}}^2 \rangle = 2 \left(\frac{\hbar \omega_1^{(\text{at})}}{\epsilon_0 V} \right) \left| \sum_k b_k(t) \sin \left[(k_0 + k) \frac{\pi z}{L} \right] \right|^2. \quad (36)$$

(In this expression we have dropped the infinite term arising from vacuum expectation value of $\hat{\mathcal{E}}^2$.) Evaluation of $\langle \hat{\mathcal{E}}^2 \rangle$ gives a space- and time-dependent representation of the localization of the energy of the photon [14, 15, 16].

The expression for $\langle \hat{\mathcal{E}}^2 \rangle$ in Eq. (36) is the square of a complex number that is analogous to the complex analytic signal describing the classical field. We label this quantity $\tilde{\mathcal{E}}_{\text{q.m.}}$, i.e.,

$$\tilde{\mathcal{E}}_{\text{q.m.}} = \sqrt{\frac{2\hbar\omega_1^{(\text{at})}}{\epsilon_0 V}} \sum_k b_k(t) \sin \left[(k_0 + k) \frac{\pi z}{L} \right]. \quad (37)$$

We note that the quantity $\tilde{\mathcal{E}}_{\text{q.m.}}$ is effectively equivalent to $\langle 0 | \hat{E}^{(+)} | \psi_\gamma \rangle$, where $\hat{E}^{(+)}$ is the positive frequency part

of the field quantized in terms of traveling wave modes, which has been identified as “the ‘electric field’ associated with [a] single photon state” by Scully and Zubairy [12]. In a previous paper [14] we extended the quantum-classical correspondence embodied in this quantity to fields that include scattering from two-level atoms, and here we extend it to include scattering from three-level atoms that make up a medium that exhibits electromagnetically induced transparency.

For ease of comparison with previous results for the detector atom, we calculate the field at the fixed position $z = 3L/4$ in a cavity that does not contain the detector atom. With no scattering atom present we find [14]

$$\tilde{\mathcal{E}}_{\text{q.m.}}^0 = -i\Theta \left(t - \frac{1}{2} \right) \sqrt{\frac{\hbar\omega_1^{(\text{at})}\gamma_1}{2\epsilon_0 V}} e^{-\frac{\gamma_1}{2}(t-\frac{1}{2})}. \quad (38)$$

The energy density passing the point $z = 3L/4$ exhibits an abrupt turn-on (because of the initial conditions we have chosen) followed by exponential decay [12, 14, 15, 16]. With a three-level scattering atom present at $z = L/2$ we find

$$\begin{aligned} \tilde{\mathcal{E}}_{\text{q.m.}} = & -i\Theta \left(t - \frac{1}{2} \right) \sqrt{\frac{\hbar\omega_1^{(\text{at})}\gamma_1}{2\epsilon_0 V}} \left\{ e^{-\frac{\gamma_1}{2}(t-\frac{1}{2})} + \frac{\gamma_2(\gamma_1 + i2\delta)e^{-\frac{\gamma_1}{2}(t-\frac{1}{2})}}{\gamma_1^2 - \gamma_1\gamma_2 - 4\delta^2 + \omega_R^2 + i2\delta(2\gamma_1 - \gamma_2)} \right. \\ & + \frac{\gamma_2 \left(\gamma_2 - \sqrt{\gamma_2^2 - 4\omega_R^2} \right) e^{[-(\gamma_2 - \sqrt{\gamma_2^2 - 4\omega_R^2})/4 + i\delta](t-\frac{1}{2})}}{\sqrt{\gamma_2^2 - 4\omega_R^2} (2\gamma_1 - \gamma_2 + \sqrt{\gamma_2^2 - 4\omega_R^2} + i4\delta)} \\ & \left. + \frac{\gamma_2 \left(\gamma_2 + \sqrt{\gamma_2^2 - 4\omega_R^2} \right) e^{[-(\gamma_2 + \sqrt{\gamma_2^2 - 4\omega_R^2})/4 + i\delta](t-\frac{1}{2})}}{\sqrt{\gamma_2^2 - 4\omega_R^2} (2\gamma_1 - \gamma_2 - \sqrt{\gamma_2^2 - 4\omega_R^2} + i4\delta)} \right\}. \end{aligned} \quad (39)$$

The first term in curly brackets is just the previous result with no scattering atom present; the effect of the scattering is contained in the remaining terms. The steady state scattering is contained in the second term in curly brackets. This term decays at the slow rate γ_1 reflecting the envelope of the incident radiation. We claimed previously that for large γ_3 the detector atom response reflects the field incident upon it, and comparison of Eq. (30), which gives the probability amplitude due to scattering for the detector atom, with Eq. (39), justifies this claim. In the limit $\gamma_3 \gg \gamma_2, \gamma_1$ the factors \mathcal{F}_{20} through \mathcal{F}_{23} that arise in Eq. (30) are proportional to the coefficients in front of the corresponding exponential terms in Eq. (39).

The quantum pulse of Eq. (38) has the classical analog

$$\tilde{\mathcal{E}}_{\text{cl.}}^0 = \Theta \left(t - \frac{1}{2} \right) C e^{-(\frac{\gamma_1}{2} + i\omega_1)(t-\frac{1}{2})}, \quad (40)$$

where C is a constant. If such classical pulses are incident on a thin slab of material with thickness Δz , density N , and classical susceptibility χ given by Eq. (1), then the classical transmitted field $\mathcal{E}_{\text{cl.}}$ is identical in form to Eq. (39), except that the terms due to scattering (i.e., those proportional to γ_2) have a magnitude characterized by the small dimensionless factor $N\Delta z|d|^2\omega/(\hbar\epsilon_0 c\gamma_2)$. A derivation of this result is included in an appendix.

IV. COMPARISON OF SEMI-CLASSICAL AND QUANTUM MECHANICAL SCATTERING

In the semi-classical model the result of weak scattering of a monochromatic field is contained in Eq. (4). In the limit of narrow bandwidth probe ($\gamma_1 \ll \gamma_2$) and rapid detector atom response ($\gamma_3 \gg \gamma_1, \gamma_2$) our quan-

tum probability for the detector atom to be excited by the scattered field is approximated by the first term of Eq. (30),

$$\begin{aligned} c_3^s(t) &\simeq \Theta\left(t - \frac{1}{2}\right) e^{-\frac{\gamma}{2}(t-\frac{1}{2})} \mathcal{F}_{20} \\ &\simeq -\Theta\left(t - \frac{1}{2}\right) e^{-\frac{\gamma}{2}(t-\frac{1}{2})} \sqrt{\frac{\gamma_1}{\gamma_3}} \\ &\quad \times \frac{i\delta\gamma_2/2}{\omega_R^2/4 - \delta^2 - i\delta\gamma_2/2} \\ &\simeq c_3^0(t) \frac{i\delta\gamma_2/2}{\omega_R^2/4 - \delta^2 - i\delta\gamma_2/2} \end{aligned} \quad (41)$$

This is exactly the same functional form as the term due to scattering in the formula for the classical field, Eq. (4). In the classical formula the dimensionless factor $N\Delta z|d|^2\omega/(\hbar\epsilon_0 c\gamma)$ is assumed to be small. In our quantum model the magnitude of the scattering is determined by Ω_2 (or equivalently γ_2), which characterizes the coupling of atom 2 to the probe field. In our one-dimensional model the coupling to the incident field and the decay rate of atom 2 are both completely determined by the single parameter Ω_2 , which means that it is not possible to make the effect of the scattering small without simultaneously making the linewidth of atom 2 very narrow. In a fully three-dimensional model the decay rate of atom 2 would be the result of the atom's coupling to many more modes, and not just those containing the incident field. This scattering into other modes would reduce the scattering in the forward direction (the direction of the detector) from the amount predicted in our simple model. If the forward scattering is reduced by a factor f , then a more realistic expression for the excitation of the detector atom is

$$c_3(t) = c_3^0(t) + f c_3^s(t). \quad (42)$$

In this formula f plays a role analogous to the dimensionless factor $N\Delta z|d|^2\omega/(\hbar\epsilon_0 c\gamma)$ in the formulas for the transmitted field derived from semi-classical theory.

V. TEMPORAL-CENTER-OF-GRAVITY DELAY

The group velocity of a classical field has a clear interpretation for quasi-monochromatic pulses whose central frequency is far from a region of anomalous dispersion: it is the speed at which the peak of the modulation envelope travels. Group delays refer to the delay in the arrival of the peak of a pulse compared to the time expected for propagation through a vacuum. The pulses investigated in this paper have sharp leading edges, and this lack of a smooth modulation envelope means that the results of simple classical theory for quasi-monochromatic pulses should not be expected to be a sufficient guide to full understanding. In this section we will investigate “temporal-center-of-gravity” delays in several classical and quantum mechanical quantities.

The first delay we investigate is derived from $c_3(t)$, the amplitude for the detector atom to be excited. As we have argued previously, this amplitude reflects the strength of the incident field in the limit that the response time of this atom is very short compared with other time scales, i.e., $\gamma_3 \gg \gamma_1, \gamma_2$. The effect of the scattering on this amplitude is evident in Fig. 7, in which $|c_3(t)|^2$, the probability for the detector atom to be excited, is plotted for three values of the detuning δ , and also for the case in which no scattering atom is present. (The results are plotted for the specific case in which $\omega_R = \gamma_2/2$.) For all detunings, $c_3(t) = 0$ for all times earlier than $t = 0.5L/c$, as is expected; all effects on the detector atom occur at times that preserve causality. The qualitative shapes of the detector response depend critically on the detuning δ . For $\delta = 0$ the steady-state absorption coefficient is zero, and this is reflected in the fact that at large times there is little effect of the scattering on the probability. At shorter times the effect of transient oscillations have a pronounced affect, and the temporal center of gravity of the response is clearly shifted toward later times relative to that of the response with no scattering atom present. The temporal center of gravity shifts to earlier times as the detuning is increased, and for values in the vicinity $\delta = \gamma_2/2$ it occurs earlier than the in the case of no scattering. This is the region in which negative values of the group delay occur, as is illustrated in Fig. 3. The finite response time of the medium results in large brief transmission of leading edge of the pulse of the field before the high attenuation of the steady state sets in. (A similar effect occurs in scattering from simple two-level atoms [14].) At larger values of the detuning, such as the case $\delta = \gamma_2$ illustrated in the bottom graph of Fig. 7, most of the probability is again removed at early times, shifting the temporal center of mass back to later times.

We quantify the ideas illustrated in Fig. 7 by identifying an effective arrival time of the photon with the temporal center of gravity of the probability that the detector atom is excited, i.e.,

$$t_{\text{arrival}} = \frac{\int t |c_3(t)|^2 dt}{\int |c_3(t)|^2 dt}. \quad (43)$$

(In evaluating the integrals in this equation, we use only the first term in the series of Eq. (25), and assume that the decay rates and distances are such that the effect of multiple scattering is negligible.) The delay imposed by the medium is then just the difference in the arrival times calculated with and without a scattering atom present,

$$\Delta t_{c_3} = \frac{\int t |c_3(t)|^2 dt}{\int |c_3(t)|^2 dt} - \frac{\int t |c_3^0(t)|^2 dt}{\int |c_3^0(t)|^2 dt}. \quad (44)$$

To explore the effect of weak scattering we rewrite $c_3(t)$ in the form of Eq. (42), and assume that $f \ll 1$. Our quantum mechanical delay becomes, to first order in f ,

$$\Delta t_{c_3} = \frac{\int t |c_3^0(t) + f c_3^s(t)|^2 dt}{\int |c_3^0(t) + f c_3^s(t)|^2 dt} - \frac{\int t |c_3^0(t)|^2 dt}{\int |c_3^0(t)|^2 dt}$$

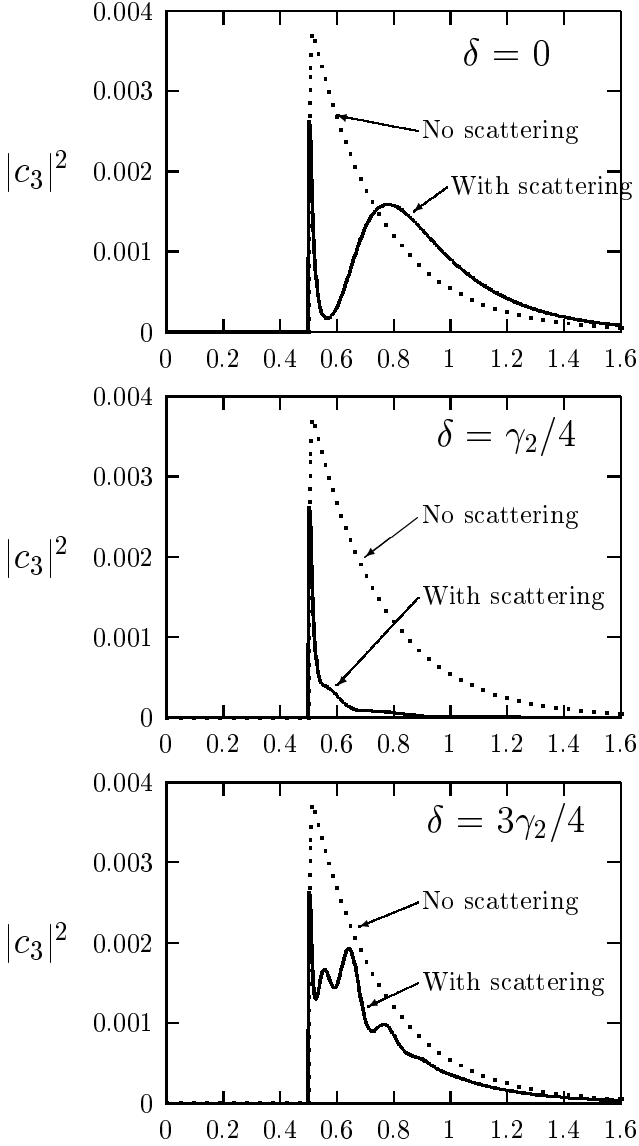


FIG. 7: Probability for the detector atom to be excited as a function of time for various values of the detuning δ . (All effects due to multiple scattering and reflections have been suppressed.) The effect of the “pulse reshaping” is dependent on the detuning. The temporal center of gravity of the probability is shifted relative to that in the case of no scattering from relatively late times in the top graph to earlier times in the middle two graphs, and then back to later times in the bottom graph. The decay rates of the atoms are $\gamma_1 = 4, \gamma_2 = 64$, and $\gamma_3 = 1024$; the Rabi frequency of the B-C transition of atom 2 is $\omega_R = \gamma_2/2 = 32$.

$$\simeq 2f \left[\frac{\int t \operatorname{Re} [c_3^0(t) c_3^s(t)^*] dt}{\int |c_3^0(t)|^2 dt} - \frac{\int t |c_3^0(t)|^2 dt \int \operatorname{Re} [c_3^0(t) c_3^s(t)^*] dt}{(\int |c_3^0(t)|^2 dt)^2} \right]. \quad (45)$$

It is straightforward (but involved) to evaluate the integrals in Eq. (45) using the expressions for $c_3^0(t)$ and $c_3^s(t)$ from Eqs. (29) and (30). After taking the limit $\gamma_3 \rightarrow \infty$ and then letting $\gamma_1 \rightarrow 0$ we arrive at the following expression for the quantum time delay:

$$\Delta t_{c_3} = 4f\gamma_2 \frac{(\omega_R^2 + 4\delta^2) [(\omega_R^2 - 4\delta^2)^2 - 4\gamma^2\delta^2]}{[(\omega_R^2 - 4\delta^2)^2 + 4\gamma^2\delta^2]^2}. \quad (46)$$

Recalling that the parameter f characterizes the magnitude of the scattering in the forward direction in the same way that the quantity $N\Delta z|d|^2\omega/(\hbar\epsilon_0 c\gamma)$ does in the semi-classical case, we see that our “temporal-center-of-gravity” delay time for this specific pulse is identical in functional form to the expression for the group delay of the classical field given in Eq. (6). The magnitude of the temporal-center-of-gravity, however, is twice that given by the group delay, i.e.,

$$\Delta t_{c_3} = 2(\Delta t_g)_{\text{classical}}. \quad (47)$$

The difference in the classical group delay and the temporal-center-of-mass delay should not be surprising, because the pulses studied in this paper do not satisfy the quasimonochromatic condition. The delay in the arrival time that we have defined is the result of the reshaping of the “pulse” of excitation of the detector atom. The effect of scattering in the region of resonance is effectively to redistribute (in time) the probability that the detector atom will be excited. The atom can rapidly absorb energy from the probe field, and the coupling field creates a state of the system which can then return energy to the probe field at a rate which can be adjusted, via the Rabi frequency ω_R , to be arbitrarily slow. Although we have not demonstrated it explicitly in this work, we are confident that delays of quasi-monochromatic quantum pulses with smooth envelopes can be explained in the same manner.

Because $\tilde{\mathcal{E}}_{\text{cl.}}$, $\tilde{\mathcal{E}}_{\text{q.m.}}$, and $c_3(t)$ all have the same functional form (in the large γ_3 limit), it is easy to see that equivalent delays can be derived from the classical field using Eq. (7), or from the quantum field using the analogous equation

$$\Delta t_{\langle \mathcal{E}^2 \rangle} = \left(\frac{\int t \langle \hat{\mathcal{E}}(z = 3L/4)^2 \rangle dt}{\int \langle \hat{\mathcal{E}}(z = 3L/4)^2 \rangle dt} \right)_{\text{with scatterer}} - \left(\frac{\int t \langle \hat{\mathcal{E}}(z = 3L/4)^2 \rangle dt}{\int \langle \hat{\mathcal{E}}(z = 3L/4)^2 \rangle dt} \right)_{\text{no scatterer}}. \quad (48)$$

VI. CONCLUSION

We have considered a fully quantized model of scattering by three-level atoms which can exhibit electromagnetically induced transparency. Our model is simple enough that we are able to find an analytical solution describing the complete dynamics of the system. Using this

model we have investigated propagation of single spontaneously emitted photons through a medium exhibiting electromagnetically induced transparency, and have defined an effective time of arrival at a detector atom. We have also calculated the expectation value of the field intensity operator, and identified a quantum analog to the complex analytic signal describing the classical field. These quantum mechanical quantities exhibit delays that are clearly the result of pulse reshaping effects. We have compared our delays for quantized one-photon fields with those calculated for classical fields using the index of refraction determined from semi-classical theory, and find them to be in agreement.

APPENDIX A: SOLUTION USING LAPLACE TRANSFORMS

Before solving the coupled differential equations resulting from the Schrödinger equation, Eqs. (17-21), we re-zero the energy scale and measure all energies relative to the energy of the initial state $|e, g, g; \emptyset\rangle$ (ignoring $\hat{H}_{\text{interaction}}$). Taking the Laplace transform of this set of coupled differential equations gives a set of coupled algebraic equations,

$$i(s\tilde{c}_1(s) - 1) = \sum_k g_{1k}\tilde{b}_k(s), \quad (\text{A1})$$

$$(is + \delta)\tilde{c}_2(s) = \sum_k g_{2k}\tilde{b}_k(s) + \omega_R\tilde{d}(s)/2, \quad (\text{A2})$$

$$is\tilde{c}_3(s) = \sum_k g_{3k}\tilde{b}_k(s), \quad (\text{A3})$$

$$is\tilde{d}(s) = \omega_R\tilde{c}_2(s)/2 - \delta\tilde{d}(s), \quad (\text{A4})$$

$$is\tilde{b}_k(s) = \sum_j g_{jk}^*\tilde{c}_j(s) + k\Delta\tilde{b}_k(s). \quad (\text{A5})$$

We solve these algebraic equations for the quantities $\tilde{c}_j(s)$, $\tilde{d}(s)$, and $\tilde{b}_k(s)$, and then perform an inverse Laplace transform to recover the time dependence of

$c_j(t)$, $d(t)$, and $b_k(t)$. The details of carrying out such calculations are quite involved, and were completed with the aid of a computer algebra system [25]. In this appendix we outline our approach and present some of our intermediate results.

We begin by solving Eq. (A4) for $\tilde{d}(s)$ and Eq. (A5) for $\tilde{b}_k(s)$, and substitute the results in the first three equations, giving

$$s\tilde{c}_1 - 1 = -i\Delta(f_{11}\tilde{c}_1 + f_{12}\tilde{c}_2 + f_{13}\tilde{c}_3), \quad (\text{A6})$$

$$\begin{aligned} \tilde{c}_2 = & -i\Delta(f_{12}\tilde{c}_1 + f_{22}\tilde{c}_2 + f_{23}\tilde{c}_3) \\ & \times \left[\frac{4(s - i\delta)}{4(s - i\delta)^2 + \omega_R^2} \right], \end{aligned} \quad (\text{A7})$$

$$s\tilde{c}_3 = -i\Delta(f_{13}\tilde{c}_1 + f_{23}\tilde{c}_2 + f_{33}\tilde{c}_3), \quad (\text{A8})$$

in which we have defined the dimensionless sums

$$f_{lm} = \frac{1}{\Delta^2} \sum_k \frac{g_{lk}g_{mk}^*}{\frac{is}{\Delta} - k}. \quad (\text{A9})$$

In the limit in which the atomic resonance frequencies are very much greater than the fundamental frequency of the cavity, i.e., $\omega_j^{(\text{at})} \gg \Delta$, these sums may be approximated by extending the range for k from $-\infty$ to $+\infty$, in which case the sums have relatively simple representations in terms of trigonometric functions. Explicit expressions for these sums are given in the Appendix of Ref. [14].

After solving Eqs. (A6-A8) for the quantities $\tilde{c}_j(s)$ in terms of the sums f_{jk} , we rewrite the hyperbolic trigonometric functions resulting from the sums in terms of exponential functions, and expand the resulting expressions in powers of $\exp(-s/2)$ or $\exp(-s/4)$. We also let $c/L = 1$ at this point in the calculation. The time dependence of the system is recovered by a term-by-term inverse Laplace transform of the expansion. The step function turn-on of the resulting time dependence arises because of the factors $\exp(-ns/4)$ in the expansion. The lowest order terms in our expansions of the Laplace transforms are given here:

$$\tilde{c}_1(s) = \frac{2}{2s + \gamma_1} + \frac{2e^{-s/2}\gamma_1[4s^2 + 4s\gamma_2 - 4\delta^2 + \omega_R^2 - 4i\delta(2s + \gamma_2)]}{(2s + \gamma_1)^2[4s^2 + 2s(\gamma_2 - i4\delta) - i2\gamma_2\delta - 4\delta^2 + \omega_R^2]} + \dots \quad (\text{A10})$$

$$\tilde{c}_2(s) = -\frac{4e^{-s/4}\sqrt{\gamma_1\gamma_2}(s - i\delta)}{(2s + \gamma_1)[4s^2 + 2s\gamma_2 - 4\delta^2 + \omega_R^2 - i2\delta(4s + \gamma_2)]} + \dots \quad (\text{A11})$$

$$\tilde{c}_3(s) = -\frac{2e^{-s/2}\sqrt{\gamma_1\gamma_3}(4s^2 - 4\delta^2 + \omega_R^2 - i8s\delta)}{(2s + \gamma_1)(2s + \gamma_3)[4s^2 + 2s\gamma_2 - 4\delta^2 + \omega_R^2 - i2\delta(4s + \gamma_2)]} + \dots \quad (\text{A12})$$

$$\tilde{d}(s) = \frac{i2e^{-s/4}\sqrt{\gamma_1\gamma_2}\omega_R}{(2s + \gamma_1)[4s^2 + 2s\gamma_2 - 4\delta^2 + \omega_R^2 - i2\delta(4s + \gamma_2)]} + \dots \quad (\text{A13})$$

$$\tilde{b}_k(s) = -\frac{i2g_{1k}}{(s+ik\pi)(2s+\gamma_1)} + \frac{i4e^{-s/4}\sqrt{\gamma_1\gamma_2}(s-i\delta)g_{2k}}{(s+ik\pi)(2s+\gamma_1)[4s^2+2s\gamma_2-4\delta^2+\omega_R^2-i2\delta(4s+\gamma_2)]} + \dots \quad (\text{A14})$$

The inverse Laplace transform of these expressions gives Eqs. (23–27).

APPENDIX B: COEFFICIENTS IN ANALYTICAL SOLUTION

The coefficients that appear in Eqs. (23-27) are given by the following expressions:

$$\mathcal{F}_1 = \frac{\gamma_1\gamma_2(-\gamma_1^2+4\delta^2+\omega_R^2-i4\gamma_1\delta)}{[\gamma_1^2-\gamma_1\gamma_2-4\delta^2+\omega_R^2+i2\delta(2\gamma_1-\gamma_2)]} \quad (\text{B1})$$

$$\mathcal{F}_2 = \frac{\gamma_1[\gamma_1^2-\gamma_1\gamma_2-4\delta^2+\omega_R^2+i2\delta(2\gamma_1-\gamma_2)][\gamma_1^2-2\gamma_1\gamma_2-4\delta^2+\omega_R^2+i4\delta(\gamma_1-\gamma_2)]}{2[\gamma_1^2-\gamma_1\gamma_2-4\delta^2+\omega_R^2+i\delta(2\gamma_1-\gamma_2)]} \quad (\text{B2})$$

$$\mathcal{F}_3 = \frac{2\gamma_1\gamma_2(-\gamma_2+\sqrt{\gamma_2^2-4\omega_R^2})}{\sqrt{\gamma_2^2-4\omega_R^2}(2\gamma_1-\gamma_2+\sqrt{\gamma_2^2-4\omega_R^2}+i4\delta)^2} \quad (\text{B3})$$

$$\mathcal{F}_4 = \frac{2\gamma_1\gamma_2(\gamma_2+\sqrt{\gamma_2^2-4\omega_R^2})}{\sqrt{\gamma_2^2-4\omega_R^2}(-2\gamma_1+\gamma_2+\sqrt{\gamma_2^2-4\omega_R^2}-i4\delta)^2} \quad (\text{B4})$$

$$\mathcal{F}_5 = \frac{\sqrt{\gamma_1\gamma_2}(\gamma_1+i2\delta)}{\gamma_1^2-\gamma_1\gamma_2-4\delta^2+\omega_R^2+i2\delta(2\gamma_1-\gamma_2)} \quad (\text{B5})$$

$$\mathcal{F}_6 = \frac{\sqrt{\gamma_1\gamma_2}(\gamma_2-\sqrt{\gamma_2^2-4\omega_R^2})}{\sqrt{\gamma_2^2-4\omega_R^2}(2\gamma_1-\gamma_2+\sqrt{\gamma_2^2-4\omega_R^2}+i4\delta)} \quad (\text{B6})$$

$$\mathcal{F}_7 = \frac{\sqrt{\gamma_1\gamma_2}(\gamma_2+\sqrt{\gamma_2^2-4\omega_R^2})}{\sqrt{\gamma_2^2-4\omega_R^2}(-2\gamma_1+\gamma_2+\sqrt{\gamma_2^2-4\omega_R^2}-i4\delta)} \quad (\text{B7})$$

$$\mathcal{F}_8 = \frac{4\sqrt{\gamma_1\gamma_3}(\gamma_1^2-4\delta^2+\omega_R^2+i4\gamma_1\delta)}{(\gamma_3-\gamma_1)(2\gamma_1-\gamma_2+\sqrt{\gamma_2^2-4\omega_R^2}+i4\delta)(-2\gamma_1+\gamma_2+\sqrt{\gamma_2^2-4\omega_R^2}-i4\delta)} \quad (\text{B8})$$

$$\mathcal{F}_9 = -\frac{2\sqrt{\gamma_1\gamma_3}\gamma_2(\gamma_2-\sqrt{\gamma_2^2-4\omega_R^2})}{\sqrt{\gamma_2^2-4\omega_R^2}(2\gamma_1-\gamma_2+\sqrt{\gamma_2^2-4\omega_R^2}+i4\delta)(-\gamma_2+2\gamma_3+\sqrt{\gamma_2^2-4\omega_R^2}+i4\delta)} \quad (\text{B9})$$

$$\mathcal{F}_{10} = \frac{2\sqrt{2\gamma_1\gamma_3}\gamma_2(\gamma_2+\sqrt{\gamma_2^2-4\omega_R^2})}{\sqrt{\gamma_2^2-4\omega_R^2}(-2\gamma_1+\gamma_2+\sqrt{\gamma_2^2-4\omega_R^2}-i4\delta)(\gamma_2-2\gamma_3+\sqrt{\gamma_2^2-4\omega_R^2}-i4\delta)} \quad (\text{B10})$$

$$\mathcal{F}_{11} = -\frac{4\sqrt{\gamma_1\gamma_3}[\gamma_3+i(2\delta+\omega_R)][\gamma_3+i(2\delta-\omega_R)]}{(\gamma_3-\gamma_1)(-\gamma_2+2\gamma_3+\sqrt{\gamma_2^2-4\omega_R^2}+i4\delta)(\gamma_2-2\gamma_3+\sqrt{\gamma_2^2-4\omega_R^2}-i4\delta)} \quad (\text{B11})$$

$$\mathcal{F}_{12} = i\frac{\sqrt{\gamma_1\gamma_2}\omega_R}{\gamma_1^2-\gamma_1\gamma_2-4\delta^2+\omega_R^2+i2\delta(2\gamma_1-\gamma_2)} \quad (\text{B12})$$

$$\mathcal{F}_{13} = i\frac{2\sqrt{\gamma_1\gamma_2}\omega_R}{\sqrt{\gamma_2^2-4\omega_R^2}(2\gamma_1-\gamma_2+\sqrt{\gamma_2^2-4\omega_R^2}+i4\delta)} \quad (\text{B13})$$

$$\mathcal{F}_{14} = i\frac{2\sqrt{\gamma_1\gamma_2}\omega_R}{\sqrt{\gamma_2^2-4\omega_R^2}(-2\gamma_1+\gamma_2+\sqrt{\gamma_2^2-4\omega_R^2}-i4\delta)} \quad (\text{B14})$$

$$\mathcal{F}_{15} = i \frac{2}{\gamma_1 - i2k\pi} \quad (\text{B15})$$

$$\mathcal{F}_{16} = -i \frac{8\sqrt{\gamma_1\gamma_2}(\gamma_1 + i2\delta)}{(\gamma_1 - i2k\pi) \left(2\gamma_1 - \gamma_2 + \sqrt{\gamma_2^2 - 4\omega_R^2} + i4\delta\right) \left(-2\gamma_1 + \gamma_2 + \sqrt{\gamma_2^2 - 4\omega_R^2} - i4\delta\right)} \quad (\text{B16})$$

$$\mathcal{F}_{17} = - \frac{16\sqrt{\gamma_1\gamma_2}(\delta + k\pi)}{(\gamma_1 - i2k\pi) \left[-\gamma_2 + \sqrt{\gamma_2^2 - 4\omega_R^2} + i4(\delta + k\pi)\right] \left[\gamma_2 + \sqrt{\gamma_2^2 - 4\omega_R^2} - i4(\delta + k\pi)\right]} \quad (\text{B17})$$

$$\mathcal{F}_{18} = i \frac{4\sqrt{\gamma_1\gamma_2} \left(-\gamma_2 + \sqrt{\gamma_2^2 - 4\omega_R^2}\right)}{\sqrt{\gamma_2^2 - 4\omega_R^2} \left[-\gamma_2 + \sqrt{\gamma_2^2 - 4\omega_R^2} + i4(\delta + k\pi)\right] (2\gamma_1 - \gamma_2 + \sqrt{\gamma_2^2 - 4\omega_R^2} + i4\delta)} \quad (\text{B18})$$

$$\mathcal{F}_{19} = i \frac{4\sqrt{\gamma_1\gamma_2} \left(\gamma_2 + \sqrt{\gamma_2^2 - 4\omega_R^2}\right)}{\sqrt{\gamma_2^2 - 4\omega_R^2} \left[\gamma_2 + \sqrt{\gamma_2^2 - 4\omega_R^2} - i4(\delta + k\pi)\right] (-2\gamma_1 + \gamma_2 + \sqrt{\gamma_2^2 - 4\omega_R^2} - i4\delta)} \quad (\text{B19})$$

APPENDIX C: CLASSICAL SCATTERING OF EXPONENTIAL PULSES

A general pulse $E(z, t)$ may be written in terms of its Fourier transform as

$$E(z, t) = \frac{1}{\sqrt{2\pi}} \int_{-\infty}^{\infty} A(\omega) e^{i(k(\omega)z - \omega t)} d\omega, \quad (\text{C1})$$

where

$$A(\omega) = \frac{1}{\sqrt{2\pi}} \int_{-\infty}^{\infty} E(0, t) e^{i\omega t} dt. \quad (\text{C2})$$

We consider an incident pulse like that of Eq. (40) which for convenience we consider to arrive at the origin $z = 0$

at $t = 0$. The Fourier transform of this pulse is

$$A(\omega) = \frac{1}{\sqrt{2\pi}} \frac{1}{[\gamma_1/2 - i(\omega - \omega_1)]}. \quad (\text{C3})$$

The effect of weak scattering on a Fourier component of a plane wave is contained in Eq. (4), and we construct the transmitted pulse to the right of the scattering region from the original Fourier components appropriately modified according to this equation. Weak scattering means that the dimensionless parameter $N\Delta z|d|^2\omega/(\hbar\epsilon_0 c\gamma_2)$ is small, and for convenience we label this parameter f . The transmitted field is thus

$$\begin{aligned} E_t(z, t) &= \frac{1}{\sqrt{2\pi}} \int_{-\infty}^{\infty} A(\omega) e^{i\omega(z/c - t)} \left[1 + if \frac{\delta\gamma_2/2}{\omega_R^2/4 - \delta^2 - i\delta\gamma_2/2}\right] d\omega \\ &= \frac{C}{2\pi} \int_{-\infty}^{\infty} \frac{1}{[\gamma_1/2 - i(\omega - \omega_1)]} e^{i\omega(z/c - t)} \left[1 + if \frac{(\omega - \omega_2)\gamma_2/2}{\omega_R^2/4 - (\omega - \omega_2)^2 - i(\omega - \omega_2)\gamma_2/2}\right] d\omega \\ &= E_i(z, t) + \frac{Cif\gamma_2}{4\pi} \int_{-\infty}^{\infty} \frac{1}{[\gamma_1/2 - i(\omega - \omega_1)]} e^{i\omega(z/c - t)} \left[\frac{(\omega - \omega_2)}{\omega_R^2/4 - (\omega - \omega_2)^2 - i(\omega - \omega_2)\gamma_2/2}\right] d\omega. \end{aligned} \quad (\text{C4})$$

The integral in the last line above gives the scattered field $E_s(z, t)$. We evaluate the integral using contour integration, and note that all three poles are in the lower half of the complex plane. For $(z/c - t) > 0$ the integration

along the real axis is closed in the upper-half plane, giving a result of zero; for $(z/c - t) < 0$ the contour is closed in the lower half plane encircling the poles. Evaluating this integral gives

$$\begin{aligned}
E_s(z, t) = Cf\gamma_2 e^{-i\omega_1 t} & \left\{ \frac{(\gamma_1 + i2\delta)e^{-\frac{\gamma_1}{2}(t-z/c)}}{[\gamma_1^2 - \gamma_1\gamma_2 - 4\delta^2 + \omega_R^2 + i2\delta(2\gamma_1 - \gamma_2)]} + \frac{(\gamma_2 - \sqrt{\gamma_2 - 4\omega_R^2})e^{[-(\gamma_2 - \sqrt{\gamma_2 - 4\omega_R^2})/4 + i\delta](t-z/c)}}{\sqrt{\gamma_2^2 - 4\omega_R^2}(2\gamma_1 - \gamma_2 + \sqrt{\gamma_2^2 - 4\omega_R^2} + i4\delta)} \right. \\
& \left. + \frac{(\gamma_2 + \sqrt{\gamma_2 - 4\omega_R^2})e^{[-(\gamma_2 + \sqrt{\gamma_2 - 4\omega_R^2})/4 + i\delta](t-z/c)}}{\sqrt{\gamma_2^2 - 4\omega_R^2}(2\gamma_1 - \gamma_2 - \sqrt{\gamma_2^2 - 4\omega_R^2} + i4\delta)} \right\} \quad (C5)
\end{aligned}$$

This is identical in form to the terms describing the scattered field in the quantum mechanical expression Eq. (39). (The factor $e^{-i\omega_1 t}$ does not appear in Eq. (39) because of the zero chosen for the energy scale in the quantum calculations.)

ACKNOWLEDGMENTS

One of us (T.P.) would like to acknowledge support from Bucknell Physics Department Research Experiences

for Undergraduates Program (NSF Grant Number PHY-0097424).

-
- [1] M. O. Scully, Phys. Rev. Lett **67**, 1855 (1991).
 - [2] K.-J. Boller, A. Imamoglu, and S. E. Harris, Phys. Rev. Lett. **66**, 2593 (1991).
 - [3] J. E. Field, K. H. Hahn, and S. E. Harris, Phys. Rev. Lett. **67**, 3062 (1991).
 - [4] S. E. Harris, J. E. Field, and A. Kasapi, Phys. Rev. A **46**, R29 (1992).
 - [5] L. V. Hau, S. E. Harris, Z. Dutton, and C. H. Behroozi, Nature **397**, 594 (1999).
 - [6] M. M. Kash, V. A. Sautenkov, A. S. Zibrov, L. Hollberg, G. R. Welch, M. D. Lukin, Y. Rostovtsev, E. S. Fry, and M. O. Scully, Phys. Rev. Lett. **82**, 5229 (1999).
 - [7] L. J. Wang, A. Kuzmich, and A. Dogariu, Nature **406**, 277 (2000).
 - [8] A. Dogariu, A. Kuzmich, and L. J. Wang, Phys. Rev. A **63**, 053806 (2001).
 - [9] M. Lukin and A. Imamoglu, Nature **413**, 273 (2001).
 - [10] S. E. Harris, Phys. Today **50(7)**, 36 (1997).
 - [11] M. Lukin, S. Yellin, A. Zibrov, and M. Scully, Laser Physics **9**, 759 (1999).
 - [12] M. O. Scully and M. S. Zubairy, *Quantum Optics* (Cambridge University Press, Cambridge, 1997).
 - [13] R. P. Feynman, R. B. Leighton, and M. Sands, *The Feynman Lectures on Physics* (Addison-Wesley, Reading, MA, 1963), vol. I, chap. 31 and 32.
 - [14] T. Purdy, D. F. Taylor, and M. Ligare, quant-ph/0204009.
 - [15] M. Ligare and R. Oliveri, Am. J. Phys. **70**, 58 (2002).
 - [16] V. Bužek, G. Drobný, M. G. Kim, M. Havukainen, and P. L. Knight, Phys. Rev. A **60**, 582 (1999).
 - [17] M. Ligare and D. F. Taylor (2001), paper presented at the Eighth Rochester Conference on Coherence and Quantum Optics, URL <http://www.eg.bucknell.edu/physics/ligare.html/>.
 - [18] D. F. Taylor, Undergraduate Honors Thesis, Bucknell University (2001).
 - [19] R. L. Smith, Am. J. Phys. **38**, 978 (1970).
 - [20] S. C. Bloch, Am. J. Phys. **45**, 538 (1977).
 - [21] G. C. Stey and R. W. Gibberd, Physica **60**, 1 (1972).
 - [22] P. W. Milonni and P. L. Knight, Phys. Rev. A **10**, 1096 (1974).
 - [23] P. W. Milonni and P. L. Knight, Phys. Rev. A **11**, 1090 (1975).
 - [24] P. Meystre and M. Sargent, *Elements of Quantum Optics* (Springer, Berlin, 1999).
 - [25] Mathematica notebooks used to perform the calculations are available from the authors.